BJR

Received: 1 February 2016 | Revised: 14 August 2016 | Accepted: 19 September 2016

http://dx.doi.org/10.1259/bjr.20160109

Cite this article as:
Moon SH, Cho YS, Son Y-I, Ahn YC, Ahn M-J, Choi JY, et al. Value of ^{18}F-FDG heterogeneity for discerning metastatic from benign lymph nodes in nasopharyngeal carcinoma patients with suspected recurrence. *Br J Radiol* 2016; **89**: 20160109.

FULL PAPER

Value of ^{18}F-FDG heterogeneity for discerning metastatic from benign lymph nodes in nasopharyngeal carcinoma patients with suspected recurrence

[1]SEUNG HWAN MOON, MD, [1]YOUNG SEOK CHO, MD, [2]YOUNG-IK SON, MD, [3]YONG CHAN AHN, MD, [4]MYUNG-JU AHN, MD, [1]JOON YOUNG CHOI, MD, [1]BYUNG-TAE KIM, MD and [1]KYUNG-HAN LEE, MD

[1]Department of Nuclear Medicine, Samsung Medical Center, Sungkyunkwan University School of Medicine, Seoul, South Korea
[2]Department of Otorhinolaryngology–Head and Neck Surgery, Samsung Medical Center, Sungkyunkwan University School of Medicine, Seoul, South Korea
[3]Department of Radiation Oncology, Samsung Medical Center, Sungkyunkwan University School of Medicine, Seoul, South Korea
[4]Division of Hematology–Oncology, Department of Medicine, Samsung Medical Center, Sungkyunkwan University School of Medicine, Seoul, South Korea

Address correspondence to: Dr Kyung-Han Lee
E-mail: *khnm.lee@samsung.com*

Objective: This study investigated the value of fluorine-18 fludeoxyglucose (^{18}F-FDG) heterogeneity as an indicator of metastatic lymph nodes (LNs) in patients with nasopharyngeal carcinoma (NPC). We further assessed whether addition of this parameter improves diagnostic performance beyond that provided by maximum standardized uptake value (SUV_{max}).
Methods: We analyzed 74 LNs that were suspicious for metastasis. These LNs were measured for coefficient of variation (CV) of ^{18}F-FDG uptake, which was used as a parameter for ^{18}F-FDG heterogeneity.
Results: Multivariate logistic regression analyses revealed that a high CV (hazard ratio, 20.97; 95% confidence interval, 2.26–194.62; $p = 0.007$) was an independent predictor of metastatic LNs. However, receiver-operating characteristic curve analysis ($p = 0.278$) and net reclassification ($p = 0.539$) were unable to show improved diagnostic performance by addition of CV to SUV_{max}.
Conclusion: High CV of ^{18}F-FDG uptake is an independent risk factor for metastatic LNs in patients with NPC displaying suspicious LNs following treatment.
Advances in knowledge: Heterogeneity of ^{18}F-FDG uptake has a potential as a biomarker of metastatic LNs.

INTRODUCTION

Nasopharyngeal carcinoma (NPC) is a cancer of the head and neck with unique epidemiologic, biologic and clinical characteristics.[1] High incidence of disease recurrence, which ranges from 15 to 58%,[1–3] is an important clinical feature of this disease.[1] Recent advances in treatment techniques and strategies are providing an opportunity to potentially cure some patients with recurrent NPC.[4] Therefore, prompt identification of recurrence is of paramount importance during follow-up of patients with NPC.[5]

Fluorine-18 fludeoxyglucose (^{18}F-FDG) positron emission tomography (PET) has an important role in the diagnosis and management of NPC.[5,6] This diagnostic modality is useful for detecting metastatic disease, defining the extent of neck nodal disease and evaluating treatment response.[6] Above all, ^{18}F-FDG PET is the modality of choice for identifying and differentiating recurrence from post-radiation change.[5] Meta-analyses comparing the performance of ^{18}F-FDG PET, CT and MRI have reported a superior diagnostic accuracy of PET for detecting recurrence.[7] However, there remain limitations in identifying recurrence by ^{18}F-FDG uptake alone.[8,9] Novel parameters of FDG PET may therefore improve the diagnostic accuracy for detecting NPC recurrence.

Recently, ^{18}F-FDG heterogeneity has been shown to help predict overall outcome in patients with cancers of the head and neck,[10] oesophagus[11] and lung.[12] Indeed, heterogeneity of ^{18}F-FDG uptake may have potential as a marker for distinguishing malignant from benign lymph nodes (LNs).[13] However, the value of ^{18}F-FDG heterogeneity in NPC has not been explored. Furthermore, much less is known regarding the diagnostic role of this parameter in suspected LNs.

In this study, we thus investigated the role of ^{18}F-FDG heterogeneity as an independent marker for metastatic LNs in patients with NPC who displayed suspicious LNs on follow-up PET/CT. We further determined whether addition of this parameter improves LN characterization beyond that provided by maximum standardized uptake value (SUV_{max}) and short-axis diameters.

METHODS AND MATERIALS

Subjects

Study subjects were selected from 282 patients with pathology-proven NPC who had received radiotherapy or chemoradiotherapy and underwent ^{18}F-FDG PET/CT imaging between January 2008 and November 2013 for surveillance purpose. Follow-up of patients after treatment included clinical examination with neck CT and/or PET/CT performed every 3–6 months. Other additional diagnostic work-ups were performed at the physician discretion if clinically indicated. Recurrence or distant metastasis was diagnosed based on positive biopsy results or clinical and/or radiographic evidence of progression.

Among these cases, a total of 51 PET/CT scans (of 41 patients) that showed newly appeared or growing regional LNs that were judged by two experienced nuclear medicine physicians to require tissue confirmation, further work-up or close follow-up were included in the study. None of these patients had other malignancy at the time of PET/CT. The institutional review board approved this retrospective cohort study, and the requirement to obtain informed consents was waived.

Positron emission tomography/CT imaging

All patients fasted for at least 6 h before PET/CT studies, and blood glucose levels were <200 mg dl^{-1} at the time of ^{18}F-FDG injection. Imaging was performed on a GE STE scanner (GE Healthcare, Milwaukee, WI; 35 scans) or a GE Discovery LS scanner (GE Healthcare, Milwaukee, WI; 16 scans). At 45 min after injection of 370 MBq ^{18}F-FDG, CT images were acquired first using a 16-slice helical CT (140 KeV, 30–170 mAs with an Auto A mode; section width of 3.75 mm) with an STE scanner or an 8-slice helical CT (140 KeV, 40–120 mAs adjusted to body weight; section width of 5 mm) with an LS scanner. No i.v. or oral contrast materials were used. Emission PET images were then acquired from thigh to head for 2.5 min per frame in three-dimensional mode with an STE scanner or 4 min per frame in two-dimensional mode with an LS scanner. Attenuation-corrected PET images (voxel size, $3.9 \times 3.9 \times 3.3$ mm with STE; $4.3 \times 4.3 \times 3.9$ mm with LS) were reconstructed using CT data by an ordered-subsets expectation maximization algorithm (20 subsets, 2 iterations with STE; 28 subsets, 2 iterations with LS).

Image analysis

All PET/CT images were analyzed by experienced nuclear medicine physicians blinded to the patient history, biopsy result and how LN appearances changed on follow-up image studies using volume viewer software on a Xeleris^{TM} workstation (GE Healthcare, Milwaukee, WI). The software provides an automatically delineated volume of interest (VOI) using an standardized uptake value (SUV)-based isocontour threshold method[14] (Figure 1). LN volume contour was determined by a 41% of SUV_{max} adaptive threshold, which adapts the threshold relative to the local average background.[15–17] From the VOI, SUV_{max}, mean SUV and standard deviation (SD) of SUV were automatically obtained. The coefficient of variation (CV), defined as the ratio of the SD of SUV to mean SUV, was adopted as a parameter for ^{18}F-FDG heterogeneity. In addition, CT images of PET/CT provided short-axis diameters of LNs and information on the presence or absence of LN fatty hilum.

Lymph node status determination

Whether an LN of interest was malignant or benign was determined by pathologic confirmation or clinical or radiographic evidence of progression. LNs were classified as metastatic if confirmed by biopsy or if there was an increase in size or ^{18}F-FDG uptake of the LN on follow-up imaging studies that led to change in management plan. All other LNs, which showed the radiographic evidence of remission on the following imaging studies, were classified as benign. LN stations were assigned according to the classification proposed by the American Head and Neck Society and the American Academy of Otolaryngology—Head and Neck Surgery.[18]

Figure 1. Fludeoxyglucose (FDG) positron emission tomography (PET)/CT images of a 72-year-old male patient with nasopharyngeal carcinoma who underwent concurrent chemoradiotherapy: focally increased FDG uptake is well visualized in the left neck on the maximum-intensity projection image (a) (black arrow) and the enlarged cervical lymph node (LN) located at the left neck Level II is shown on the transverse CT image (b) (white arrow). Automatic volume of interest (VOI) using an isocontour threshold method was placed over the LN. Segmented VOIs are shown on the transverse PET image (c).

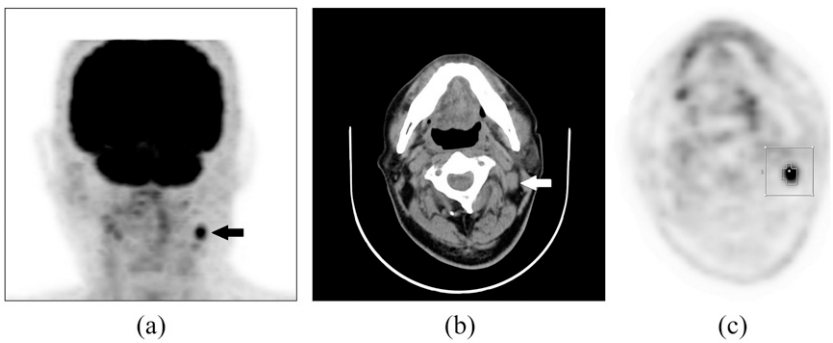

Statistical analysis

Difference between groups was compared with Mann–Whitney *U*-tests for continuous variables and χ^2 tests for dichotomous variables. Specificity, sensitivity and accuracy of parameters for discriminating metastatic LNs were compared by McNemar's tests. Optimal cut-off values for discerning metastatic LNs were determined by receiver-operating characteristic (ROC) curves, and diagnostic performances of parameters were compared by areas under the curve (AUCs).

Risk factors for metastatic LNs were identified by univariate and multivariate analyses using logistic regression models. Demographics, clinical variables, SUV_{max}, CV and LN short axis were assessed. Since the lack of multicollinearity between variables is a basic inviolable assumption for multiple logistic regression analysis, we performed collinearity statistics to test the multicollinearity between variables, particularly between CV and SUV_{max}.

Continuous net reclassification indices (NRI) were estimated to examine the net effect of adding parameters to the diagnostic scheme. NRI demonstrates how many patients are moved into different clinical risk categories by using a different model. Integrated discrimination improvement (IDI) indices were estimated to evaluate the capacity of parameters to discriminate between benign and malignant LNs. IDI demonstrates the difference between competing model discrimination slopes, which tell us whether adding a new factor to a prediction model can improve the discrimination and reclassification.

Determination of optimal cut-off values was performed with MedCalc® for Windows, v. 15.5 (MedCalc Software, Ostend, Belgium). NRI, IDI estimations and AUC comparisons between diagnostic models were conducted using SAS® v. 9.4 (SAS Institute, Cary, NC). The remaining analyses were performed with SPSS® for windows v. 16.0 (IBM Corp., New York, NY; formerly SPSS Inc., Chicago, IL). Two-sided *p*-values of <0.05 were considered significant.

RESULTS

Characteristics of study subjects and lymph nodes of interest

The subjects included in the study had a mean age of 50.0 ± 13.2 years (range, 12–78 years) at the time of PET/CT, and 75.6% subjects were males. 10 patients were included twice for PET/CT studies that were performed at separate occasions following treatment. On each PET/CT scan ($n = 51$), there were varying numbers of suspected LNs: 34 scans showed 1 suspected LN, 14 scans showed 2 suspected LNs and 3 scans showed 4 suspected LNs. Consequently, a total of 74 suspected LNs in 51 PET/CT scans were analyzed. The characteristics of PET/CT scan-based study subjects categorized according to LN status are summarized in Table 1. In 19 of the 51 scans, all of the suspected LNs were metastatic ($n = 28$); in 31 scans, all of the suspected LNs were benign ($n = 44$); and in the remaining 1 scan, 1 suspected LN was metastatic while the other was benign. The groups with "all metastatic LNs" and "all benign LNs" differed in prior history of recurrence (Table 1).

The 74 suspected LNs had a mean SUV_{max} of 4.7 ± 3.3 (range, 1.7–22.8), CV of 0.18 ± 0.04 (range, 0.11–0.25) and short-axis diameter of 7.8 ± 2.7 mm (range, 5–17.6 mm). The characteristics of metastatic and benign LNs in our study are summarized in Table 2. Metastatic LNs had significantly greater SUV_{max}, CV and short-axis diameter than benign LNs. The frequent metastatic sites were Level II cervical LN and retropharyngeal LN (Table 2). The majority of LNs showed loss of fatty hilum on CT images (68/74, 91.9%). Histopathologic examination was performed in 38 (51.3%) of 74 LNs.

Diagnostic performance of positron emission tomography/CT parameters

On ROC analysis, the AUC of PET/CT performance for diagnosing metastasis was 0.871 for SUV_{max}, 0.855 for CV and 0.778 for short-axis diameter (Supplementary Figure A). The AUC for SUV_{max} showed a trend of being greater than that of short-axis diameter, although this did not reach statistical significance ($p = 0.088$). Optimal cut-off values of SUV_{max}, CV and short-axis diameter were 4.5, 0.194 and 6.7 mm, respectively. Using these cut-off values, LNs were categorized as having low or high parameters, with which the performance of identifying metastatic involvement was assessed (Table 3). McNemar's test results demonstrated that a high SUV_{max} (≥4.6) and high CV (≥0.194) had better performance in determining LN metastasis compared with a large size (≥6.8 mm). High SUV_{max} and high CV showed higher specificity and positive-predictive values. However, there was no significant difference in performance between high SUV_{max} and high CV ($p = 0.508$).

Risk factors for metastatic lymph node

On univariate analysis, the logistic regression model demonstrated significant associations of metastatic LN with high SUV_{max} (≥4.6), high CV (≥0.194), large size (≥6.8 mm), female gender, first line of treatment, nodal staging (0,1 *vs* 2,3) and location (Table 4). Prior history of recurrence showed marginal significance, and other factors failed to show significant association with metastatic LN.

Multivariate analysis performed with significant univariate factors revealed high CV [hazard ratio (HR), 20.97; 95% confidence interval (CI), 2.26–194.62; $p = 0.007$], female gender (HR, 21.48; 95% CI, 2.38–193.93; $p = 0.006$) and location (HR, 8.89; 95% CI, 1.10–71.74; $p = 0.04$) as significant independent risk factors for metastatic LN (Table 4). Collinearity statistics showed that variance inflation factor was <10. Tolerance, another collinearity indicator, was >0.1 between significant univariate variables. These findings indicate that collinearity is not likely to have significantly affected the results of this study (data not shown).

In addition, results of subgroup analysis performed in pathologically confirmed patient group showed that high CV and female gender have significant association with metastatic LN (Supplemental Table A).

Diagnostic value and net reclassification

We next performed ROC analysis with AUC measurements to compare the discrimination capacities of models for metastatic LN. This included SUV_{max} at baseline with or without addition

Table 1. Characteristics of study subjects based on fluorine-18 fludeoxyglucose positron emission tomography (PET)/CT scans ($n = 51$)

Patient characteristics	Classification of scans according to LN status			p-value[a]
	All metastatic ($n = 19$)	All benign ($n = 31$)	Mixed ($n = 1$)	
Number of suspected LNs	28	44	2	
Number of subjects[b]	11[c]	29[c]	1	
Age (years)	50.1 ± 13.4	50.9 ± 14.4	49.0	0.841
Male, *n* (%)	12 (63.2)	25 (80.6)	1 (100.0)	0.199
Histology of primary tumour				
Differentiated, *n* (%)	03 (15.8)	07 (22.6)	–	0.272
Non-keratinizing, *n* (%)	06 (31.6)	04 (12.9)	–	
Undifferentiated, *n* (%)	10 (52.6)	20 (64.5)	1 (100.0)	
Stage at initial diagnosis				
I, *n* (%)	1 (05.3)	03 (09.7)	–	0.606
II, *n* (%)	2 (10.5)	06 (19.3)	1 (100.0)	
III, *n* (%)	8 (42.1)	10 (32.3)	–	
IV, *n* (%)	8 (42.1)	12 (38.7)	–	
First line of treatment				
CCRT, *n* (%)	11 (57.9)	23 (74.2)	1 (100.0)	0.145
Chemotherapy only, *n* (%)	05 (26.3)	02 (06.5)	0 (000.0)	
Radiation therapy only, *n* (%)	03 (15.8)	06 (19.3)	0 (000.0)	
Prior history of recurrence, *n* (%)	10 (52.6)	7 (22.6)	0 (000.0)	0.037
Follow-up duration, median (months) (range)	45.1 (2.3–9.2)	35.3 (8.4–86.4)		0.623

CCRT, concurrent chemoradiotherapy; LN, lymph node.
[a]Comparison between "all metastatic" and "all benign" groups.
[b]10 of the subjects had undergone 2 PET/CT studies on separate occasions included in the study.
[c]Four subjects belong to both groups; in addition, six subjects had "all metastatic" results on two separate PET/CT studies.

of CV and size information. Addition of CV to the SUV_{max} model did not improve diagnostic performance as measured by AUC (87.1 *vs* 89.2, $p = 0.278$) (Supplemental Table B). Addition of CV and size to the SUV_{max} model also failed to increase the AUC of diagnostic performance (87.1 *vs* 89.2, $p = 0.295$) (Supplemental Table B).

Similarly, net reclassification of performance for discerning metastatic LNs was not significantly improved by addition of CV (NRI, 3.5%; $p = 0.539$) nor by addition of CV plus size to SUV_{max} (NRI, 3.5%; $p = 0.643$) (Supplemental Table B). IDI results for adding CV and size to models including SUV_{max} are shown in Supplemental Table B.

DISCUSSION

In our study of patients with NPC undergoing surveillance PET/CT following treatment, LNs with greater ^{18}F-FDG heterogeneity, as represented by high CV, were a significant and independent indicator of metastatic involvement. In our study population, however, addition of ^{18}F-FDG heterogeneity did not significantly increase diagnostic performance beyond that provided by SUV_{max}.

Heterogeneity of ^{18}F-FDG uptake may have potential as a marker for distinguishing malignant from benign LNs.[13] Malignant tumours are composed of substantially heterogeneous tissues[19–23] and are therefore expected to have less homogeneous distribution of ^{18}F-FDG uptake compared with benign lesions. This is partly owing to the many different tumour components, which include not only cancer cells but also infiltrating inflammatory cells, vascular cells, connective stroma, granulation tissue and necrotic tissue. Indeed, breast tumours have been shown to harbour markedly divergent proportions cancer cells, ranging from only a small number of cells up to 90% of the tumour bulk.[21] Different tumour components vary in their metabolic activity[19,20] and therefore contribute differently to overall tumour ^{18}F-FDG uptake. In addition, cancer cells within the same tumour also show phenotypic and functional heterogeneity as a characteristic feature of malignant tumours.[24] Furthermore, regional tumour ^{18}F-FDG accumulation can be significantly influenced by local pathophysiological processes such as hypoxia, angiogenesis, proliferation and cell death.[25–27] Hence, heterogeneity of ^{18}F-FDG uptake could partly reflect these heterogeneous components within tumour tissue.[19–22]

Table 2. Characteristics of suspected lymph nodes (LNs) ($n = 74$)

Lymph node characteristics	Metastatic LN ($n = 29$)	Benign LN ($n = 45$)	p-value
LN location, n (%)			
Level I	001 (003.5)	07 (15.5)	0.027
Level II	011 (037.9)	03 (06.7)	
Level III	03 (010.3)	10 (22.2)	
Level IV	05 (017.2)	13 (28.9)	
Level V	02 (006.9)	02 (04.4)	
Level VI and VII	01 (003.5)	04 (08.9)	
Retropharyngeal	04 (013.8)	03 (06.7)	
Other sites	02 (006.9)	03 (06.7)	
Pathology confirmed, n (%)	23 (079.3)	15 (33.3)	<0.000
Loss of fatty hilum[a], n (%)	29 (100.0)	39 (86.7)	0.075
Short-axis diameter (mm)	9.1 ± 2.5	6.7 ± 2.7	<0.000
SUV_{max}	7.1 ± 4.3	3.3 ± 0.9	<0.000
CV	0.21 ± 0.03	0.16 ± 0.03	<0.000

CV, coefficient of variation; SUV_{max}, maximum standardized uptake value.
[a]Present in 68/74 (91.9%) of the LNs assessed.

The divergent ^{18}F-FDG avidity of tumour components and cancer cell phenotype, as well as local pathophysiological processes, can explain a possible association between histopathologic heterogeneity and distribution of ^{18}F-FDG uptake within tumours. Thus, the potential usefulness of tumour ^{18}F-FDG heterogeneity as a surrogate imaging marker for tumour heterogeneity is recently gaining increasing interest. Results to date have demonstrated significant associations between baseline tumour ^{18}F-FDG heterogeneity and overall outcome in patients with cancers of the head and neck,[10] oesophagus[11] and lung.[12] However, while these findings support the potential prognostic role of tumour ^{18}F-FDG heterogeneity, there are few data on tumour ^{18}F-FDG heterogeneity in NPC as to the best of the authors' knowledge. In addition, less is known regarding the diagnostic role of this parameter. Budiawan et al[13] assessed 94 LNs from 44 patients with treatment-naïve adenocarcinoma of the lung and observed more heterogeneous ^{18}F-FDG uptake in metastatic LNs than that in inflammatory LNs.

This study tested the value of CV, defined as SD divided by the mean value of the activity concentration in the tumour volume, as a parameter of heterogeneous ^{18}F-FDG uptake for determining metastatic involvement of LNs in patients with NPC. CV of the SUV derived from a manual VOI has previously been shown to be an independent factor for LN metastasis.[13] In the patients with NPC, the diagnostic value of tumour heterogeneity as assessed by ^{18}F-FDG PET has not been investigated. In our results, high CV was an independent risk factor associated with metastatic LNs with diagnostic performance comparable with that of SUV_{max}, the most popular and useful PET parameter to date. In our study subjects, however, addition of CV information to SUV_{max} did not significantly increase the AUC of diagnostic performance. Furthermore, NRI results did not show more appropriate reclassification of LNs by addition of CV to SUV_{max}. Estimated IDI, which indicates magnitudes of change in predicted risk, was also relatively small when CV was added to SUV_{max}. It should be noted, however, that the small number of

Table 3. Diagnostic performance of positron emission tomography/CT parameters for detecting metastasis lymph nodes

Parameters	Lesion-based results (n)					Diagnostic performance (%)					p-value
	TP	TN	FP	FN	Total	SN	SP	Accuracy	PPV	NPV	
SUV_{max} (≥4.6)	21	42	3	8	74	72.4	93.3	85.1	87.5	84.0	
Size (≥6.8 mm)	23	28	17	6	74	79.3	62.2	68.9	57.5	82.4	0.003[a]
CV (≥0.194)	22	40	5	7	74	75.9	88.9	83.8	81.5	85.1	0.508[a], 0.004[b]

CV, coefficient of variation; FN, false negative; FP, false positive; NPV, negative predictive value; PPV, positive predictive value; SN, sensitivity; SP, specificity; SUV_{max}, maximum standardized uptake value; TN, true negative; TP, true positive.
[a]compared with SUV_{max}.
[b]compared with size criteria.

Table 4. Logistic regression analysis for risk factors associated with metastatic lymph nodes

Variables	Univariate			Multivariate		
	HR	95% CI	*p*-value	HR	95% CI	*p*-value
SUV_{max} (≥4.6)	36.75	8.83–153.04	<0.000	5.45	0.47–062.73	0.174
CV (≥0.194)	25.14	7.13–088.64	<0.000	20.97	2.26–194.62	0.007
Size (≥6.8 mm)	04.71	1.67–013.32	0.003	1.30	0.07–022.60	0.859
Female gender	03.97	1.27–012.43	0.018	21.48	2.38–193.93	0.006
First line of treatment						
Chemotherapy only	05.33	1.28–022.21	0.021	2.07	0.08–050.39	0.654
Location						
Level II or retropharynx	06.96	2.26–021.49	0.001	8.89	1.10–071.74	0.04
Nodal staging (0, 1 *vs* 2, 3)	3.01	1.07–8.43	0.037	1.78	0.25–012.65	0.56
Prior history of recurrence	02.47	0.89–006.85	0.082			
Stage (I *vs*)						
II	00.83	0.11–006.11	0.858			
III	01.83	0.30–011.26	0.513			
IV	02.31	0.37–014.21	0.367			
Histology (differentiated *vs*)						
Non-keratinizing	01.56	0.33–007.36	0.577			
Undifferentiated	01.29	0.34–004.90	0.713			
Age (>50 years)	00.98	0.38–002.48	0.959			
Loss of fatty hilum	1.20×10^9	0.00–00NC	0.999			

CI, confidence interval; CV, coefficient of variation; HR, hazard ratio; NC, not calculable; SUV_{max}, maximum standardized uptake value.

subjects in this exploratory study may not have had sufficient power to detect an incremental value of tumour ^{18}F-FDG heterogeneity for diagnosis of metastatic LNs.

A number of different parameters can be used as a measure of tumour ^{18}F-FDG heterogeneity.[23] Texture analysis of images, a mathematical method that describes the relationship between grey-level intensity of pixels/voxels and their position, is recently emerging as a new tool for characterizing tumour heterogeneity.[23] Second-order or higher order textural features have shown to offer better tissue characterization and image segmentation and improve prediction of therapy response and survival.[23] Although CV may not be the most sophisticated or highest precision parameter for tissue heterogeneity, it is widely accessible and can be easily applied in routine clinical practice without the need for specialized software. Furthermore, findings based on the results of recent studies support the possible additional role of CV.[28] Calculation of baseline CV or its change between baseline and post-treatment scans may have potential utility in predicting prognosis or treatment response. Clarification of this issue could be an interesting topic for further studies regarding the prognostic value of tumour ^{18}F-FDG heterogeneity.

Another methodological issue is lesion boundary delineation on the PET/CT images, which is important because of its significant impact on measurements of the mean value of ^{18}F-FDG activity. Manual delineations can be an appropriate option, but are laborious and time-consuming. In this study, we applied an automatic boundary delineation method using an adaptive threshold of 41%, which adapts the threshold relative to the local average background.[17] Advantages of this method over fixed threshold methods include its applicability even for small lesions with low uptake by correcting for contrast between lesion and local background,[16,17] and close correlation between tumour volumes made by this method to actual values.[15]

Effect of pathologic tumour type could be a considerable issue in evaluating ^{18}F-FDG heterogeneity. In this study, subjects consisting predominantly of undifferentiated carcinoma may have impact on evaluating heterogeneity. However, differentiated and undifferentiated tumours were found to have similar CVs of 0.174 ± 0.043 and 0.185 ± 0.041, respectively ($p = 0.43$). This finding should be confirmed in further large-scale studies with different types of tumours.

The result of our study supports the potential value of ^{18}F-FDG heterogeneity for discriminating metastatic LNs in patients with NPC. However, it should be mentioned that there is currently insufficient evidence to recommend routine FDG PET-based surveillance in NPC. Further studies may help clarify the diagnostic value of ^{18}F-FDG PET for NPC under different clinical settings, such as staging work-up.

This study has several limitations. First, as mentioned above, the small number of metastasized LNs provides suboptimal statistical power for robust analysis. Also, since the enrolled subjects were highly suspected for having LN metastasis, there is potential for selection-related biases that may restrict generalization of the study results. Lastly, adaptive threshold method used for lesion delineation has a limitation. This method may be challenging for LNs located close to high-uptake regions, where it is as difficult to accurately delineate lesion boundary as in the manual delineation method. Therefore, additional studies with prospective design, a larger number of lesions and a more sophisticated method for lesion delineation are warranted to confirm the findings of this study.

In our study, high CV was an independent predictor of metastatic nodes in patients with NPC but did not have an additive effect on SUV_{max}.

ACKNOWLEDGMENTS

The authors thank Kyunga Kim and Sun-Kyu Choi of Biostatistics and Clinical Epidemiology Center, Samsung Medical Center, for their important contributions in statistical analysis.

FUNDING

This work was supported by the Basic Science Research Program through the National Research Foundation of Korea (NRF) funded by the Ministry of Education, Science and Technology (MEST) (#2012R1A1A2041354).

REFERENCES

1. Wei WI, Sham JS. Nasopharyngeal carcinoma. *Lancet* 2005; **365**: 2041–54. doi: http://dx.doi.org/10.1016/S0140-6736(05)66698-6
2. Yang TS, Ng KT, Wang HM, Wang CH, Liaw CC, Lai GM. Prognostic factors of locoregionally recurrent nasopharyngeal carcinoma—a retrospective review of 182 cases. *Am J Clin Oncol* 1996; **19**: 337–43. doi: http://dx.doi.org/10.1097/00000421-199608000-00003
3. Chang JT, See LC, Liao CT, Ng SH, Wang CH, Chen IH, et al. Locally recurrent nasopharyngeal carcinoma. *Radiother Oncol* 2000; **54**: 135–42. doi: http://dx.doi.org/10.1016/S0167-8140(99)00177-2
4. Xu T, Tang J, Gu M, Liu L, Wei W, Yang H. Recurrent nasopharyngeal carcinoma: a clinical dilemma and challenge. *Curr Oncol* 2013; **20**: e406–19. doi: http://dx.doi.org/10.3747/co.20.1456
5. Mohandas A, Marcus C, Kang H, Truong MT, Subramaniam RM. FDG PET/CT in the management of nasopharyngeal carcinoma. *AJR Am J Roentgenol* 2014; **203**: W146–57. doi: http://dx.doi.org/10.2214/AJR.13.12420
6. Law A, Peters LJ, Dutu G, Rischin D, Lau E, Drummond E, et al. The utility of PET/CT in staging and assessment of treatment response of nasopharyngeal cancer. *J Med Imaging Radiat Oncol* 2011; **55**: 199–205. doi: http://dx.doi.org/10.1111/j.1754-9485.2011.02252.x
7. Liu T, Xu W, Yan WL, Ye M, Bai YR, Huang G. FDG-PET, CT, MRI for diagnosis of local residual or recurrent nasopharyngeal carcinoma, which one is the best? A systematic review. *Radiother Oncol* 2007; **85**: 327–35. doi: http://dx.doi.org/10.1016/j.radonc.2007.11.002
8. Chan SC, Ng SH, Chang JT, Lin CY, Chen YC, Chang YC, et al. Advantages and pitfalls of 18F-fluoro-2-deoxy-D-glucose positron emission tomography in detecting locally residual or recurrent nasopharyngeal carcinoma: comparison with magnetic resonance imaging. *Eur J Nucl Med Mol Imaging* 2006; **33**: 1032–40. doi: http://dx.doi.org/10.1007/s00259-005-0054-6
9. Al-Ibraheem A, Buck A, Krause BJ, Scheidhauer K, Schwaiger M. Clinical applications of FDG PET and PET/CT in head and neck cancer. *J Oncol* 2009; **2009**: 208725. doi: http://dx.doi.org/10.1155/2009/208725
10. El Naqa I, Grigsby P, Apte A, Kidd E, Donnelly E, Khullar D, et al. Exploring feature-based approaches in PET images for predicting cancer treatment outcomes. *Pattern Recognit* 2009; **42**: 1162–71. doi: http://dx.doi.org/10.1016/j.patcog.2008.08.011
11. Tixier F, Le Rest CC, Hatt M, Albarghach N, Pradier O, Metges JP, et al. Intratumor heterogeneity characterized by textural features on baseline 18F-FDG PET images predicts response to concomitant radiochemotherapy in esophageal cancer. *J Nucl Med* 2011; **52**: 369–78. doi: http://dx.doi.org/10.2967/jnumed.110.082404
12. Cook GJ, Yip C, Siddique M, Goh V, Chicklore S, Roy A, et al. Are pretreatment 18F-FDG PET tumor textural features in non-small cell lung cancer associated with response and survival after chemoradiotherapy? *J Nucl Med* 2013; **54**: 19–26. doi: http://dx.doi.org/10.2967/jnumed.112.107375
13. Budiawan H, Cheon GJ, Im HJ, Lee SJ, Paeng JC, Kang KW, et al. Heterogeneity analysis of (18)F-FDG uptake in differentiating between metastatic and inflammatory lymph nodes in adenocarcinoma of the lung: comparison with other parameters and its application in a clinical setting. *Nucl Med Mol Imaging* 2013; **47**: 232–41. doi: http://dx.doi.org/10.1007/s13139-013-0216-6
14. Moon SH, Choi JY, Lee HJ, Son YI, Baek CH, Ahn YC, et al. Prognostic value of 18F-FDG PET/CT in patients with squamous cell carcinoma of the tonsil: comparisons of volume-based metabolic parameters. *Head Neck* 2013; **35**: 15–22. doi: http://dx.doi.org/10.1002/hed.22904
15. Cheebsumon P, Boellaard R, de Ruysscher D, van Elmpt W, van Baardwijk A, Yaqub M, et al. Assessment of tumour size in PET/CT lung cancer studies: PET- and CT-based methods compared to pathology. *EJNMMI Res* 2012; **2**: 56. doi: http://dx.doi.org/10.1186/2191-219X-2-56
16. Boellaard R, Krak NC, Hoekstra OS, Lammertsma AA. Effects of noise, image resolution, and ROI definition on the accuracy of standard uptake values: a simulation study. *J Nucl Med* 2004; **45**: 1519–27.
17. Cheebsumon P, van Velden FH, Yaqub M, Hoekstra CJ, Velasquez LM, Hayes W, et al. Measurement of metabolic tumor volume: static *versus* dynamic FDG scans. *EJNMMI Res* 2011; **1**: 35. doi: http://dx.doi.org/10.1186/2191-219X-1-35
18. Robbins KT, Clayman G, Levine PA, Medina J, Sessions R, Shaha A, et al. Neck dissection classification update: revisions proposed by the American Head and Neck Society and the American Academy of Otolaryngology-Head and Neck Surgery. *Arch Otolaryngol Head Neck Surg* 2002; **128**: 751–8. doi: http://dx.doi.org/10.1001/archotol.128.7.751
19. Kubota R, Yamada S, Kubota K, Ishiwata K, Tamahashi N, Ido T. Intratumoral distribution of fluorine-18-fluorodeoxyglucose *in vivo*: high accumulation in macrophages and granulation tissues studied by

microautoradiography. *J Nucl Med* 1992; **33**: 1972–80.

20. Brown RS, Leung JY, Fisher SJ, Frey KA, Ethier SP, Wahl RL. Intratumoral distribution of tritiated fluorodeoxyglucose in breast carcinoma: I. Are inflammatory cells important? *J Nucl Med* 1995; **36**: 1854–61.
21. Avril N, Menzel M, Dose J, Schelling M, Weber W, Jänicke F, et al. Glucose metabolism of breast cancer assessed by 18F-FDG PET: histologic and immunohistochemical tissue analysis. *J Nucl Med* 2001; **42**: 9–16.
22. Higashi K, Clavo AC, Wahl RL. Does FDG uptake measure proliferative activity of human cancer cells? *In vitro* comparison with DNA flow cytometry and tritiated thymidine uptake. *J Nucl Med* 1993; **34**: 414–19.
23. Chicklore S, Goh V, Siddique M, Roy A, Marsden PK, Cook GJ. Quantifying tumour heterogeneity in 18F-FDG PET/CT imaging by texture analysis. *Eur J Nucl Med Mol Imaging* 2013; **40**: 133–40. doi: http://dx.doi.org/10.1007/s00259-012-2247-0
24. Meacham CE, Morrison SJ. Tumour heterogeneity and cancer cell plasticity. *Nature* 2013; **501**: 328–37. doi: http://dx.doi.org/10.1038/nature12624
25. Basu S, Kwee TC, Gatenby R, Saboury B, Torigian DA, Alavi A. Evolving role of molecular imaging with PET in detecting and characterizing heterogeneity of cancer tissue at the primary and metastatic sites, a plausible explanation for failed attempts to cure malignant disorders. *Eur J Nucl Med Mol Imaging* 2011; **38**: 987–91. doi: http://dx.doi.org/10.1007/s00259-011-1787-z
26. Pugachev A, Ruan S, Carlin S, Larson SM, Campa J, Ling CC, et al. Dependence of FDG uptake on tumor microenvironment. *Int J Radiat Oncol Biol Phys* 2005; **62**: 545–53. doi: http://dx.doi.org/10.1016/j.ijrobp.2005.02.009
27. Tixier F, Groves AM, Goh V, Hatt M, Ingrand P, Le Rest CC, et al. Correlation of intratumor 18F-FDG uptake heterogeneity indices with perfusion CT derived parameters in colorectal cancer. *PLoS One* 2014; **9**: e99567. doi: http://dx.doi.org/10.1371/journal.pone.0099567
28. Bundschuh RA, Dinges J, Neumann L, Seyfried M, Zsótér N, Papp L, et al. Textural parameters of tumor heterogeneity in ^{18}F-FDG PET/CT for therapy response assessment and prognosis in patients with locally advanced rectal cancer. *J Nucl Med* 2014; **55**: 891–7. doi: http://dx.doi.org/10.2967/jnumed.113.127340